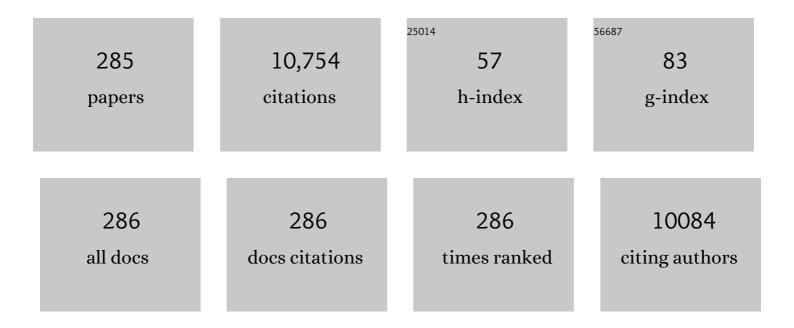
Chuan Dong

List of Publications by Year in descending order

Source: https://exaly.com/author-pdf/3270702/publications.pdf Version: 2024-02-01



#	Article	IF	CITATIONS
1	Facile synthesis of nitrogen-doped carbon dots for Fe3+ sensing and cellular imaging. Analytica Chimica Acta, 2015, 861, 74-84.	2.6	283
2	Phosphorus and Nitrogen Dual-Doped Hollow Carbon Dot as a Nanocarrier for Doxorubicin Delivery and Biological Imaging. ACS Applied Materials & Interfaces, 2016, 8, 11288-11297.	4.0	252
3	Comparative study for N and S doped carbon dots: Synthesis, characterization and applications for Fe3+ probe and cellular imaging. Analytica Chimica Acta, 2015, 898, 116-127.	2.6	208
4	An "on-off-on―fluorescent nanoprobe for recognition of chromium(VI) and ascorbic acid based on phosphorus/nitrogen dual-doped carbon quantum dot. Analytica Chimica Acta, 2017, 968, 85-96.	2.6	205
5	Highly Selective Two-Photon Fluorescent Probe for Ratiometric Sensing and Imaging Cysteine in Mitochondria. Analytical Chemistry, 2016, 88, 1908-1914.	3.2	184
6	Low temperature synthesis of phosphorous and nitrogen co-doped yellow fluorescent carbon dots for sensing and bioimaging. Journal of Materials Chemistry B, 2015, 3, 6813-6819.	2.9	144
7	One-Step Synthesis of Label-Free Ratiometric Fluorescence Carbon Dots for the Detection of Silver Ions and Glutathione and Cellular Imaging Applications. ACS Applied Materials & Interfaces, 2019, 11, 16822-16829.	4.0	137
8	Effect of Ambient PM _{2.5} on Lung Mitochondrial Damage and Fusion/Fission Gene Expression in Rats. Chemical Research in Toxicology, 2015, 28, 408-418.	1.7	133
9	Mitochondrial damage: An important mechanism of ambient PM2.5 exposure-induced acute heart injury in rats. Journal of Hazardous Materials, 2015, 287, 392-401.	6.5	127
10	Bright Yellow Fluorescent Carbon Dots as a Multifunctional Sensing Platform for the Label-Free Detection of Fluoroquinolones and Histidine. ACS Applied Materials & Interfaces, 2018, 10, 42915-42924.	4.0	121
11	Dual Photoluminescence Emission Carbon Dots for Ratiometric Fluorescent GSH Sensing and Cancer Cell Recognition. ACS Applied Materials & Interfaces, 2020, 12, 18250-18257.	4.0	118
12	Electrochemical Sensor for Ultrasensitive Determination of Doxorubicin and Methotrexate Based on Cyclodextrinâ€Graphene Hybrid Nanosheets. Electroanalysis, 2011, 23, 2400-2407.	1.5	114
13	Strategy for Activating Room-Temperature Phosphorescence of Carbon Dots in Aqueous Environments. Chemistry of Materials, 2019, 31, 7979-7986.	3.2	112
14	Folic acid-conjugated carbon dots as green fluorescent probes based on cellular targeting imaging for recognizing cancer cells. RSC Advances, 2017, 7, 42159-42167.	1.7	111
15	Folic acid-conjugated green luminescent carbon dots as a nanoprobe for identifying folate receptor-positive cancer cells. Talanta, 2018, 183, 39-47.	2.9	110
16	Sensitive electrochemical sensor for nitrite ions based on rose-like AuNPs/MoS2/graphene composite. Biosensors and Bioelectronics, 2019, 142, 111529.	5.3	110
17	Facile synthesis of orange fluorescence carbon dots with excitation independent emission for pH sensing and cellular imaging. Analytica Chimica Acta, 2018, 1042, 125-132.	2.6	108
18	Ratiometric Emission Fluorescent pH Probe for Imaging of Living Cells in Extreme Acidity. Analytical Chemistry, 2015, 87, 2788-2793.	3.2	105

#	Article	IF	CITATIONS
19	Lipid Droplet-Specific Fluorescent Probe for <i>In Vivo</i> Visualization of Polarity in Fatty Liver, Inflammation, and Cancer Models. Analytical Chemistry, 2021, 93, 8019-8026.	3.2	105
20	Controllable synthesis of green and blue fluorescent carbon nanodots for pH and Cu 2+ sensing in living cells. Biosensors and Bioelectronics, 2016, 77, 598-602.	5.3	104
21	Naked oats-derived dual-emission carbon nanodots for ratiometric sensing and cellular imaging. Sensors and Actuators B: Chemical, 2015, 210, 533-541.	4.0	97
22	Carbon nano-dots as a fluorescent and colorimetric dual-readout probe for the detection of arginine and Cu ²⁺ and its logic gate operation. Nanoscale, 2017, 9, 11545-11552.	2.8	94
23	N,S,P Co-Doped Carbon Nanodot Fabricated from Waste Microorganism and Its Application for Label-Free Recognition of Manganese(VII) and <scp>l</scp> -Ascorbic Acid and AND Logic Gate Operation. ACS Applied Materials & Interfaces, 2017, 9, 38761-38772.	4.0	93
24	β-Cyclodextrin/Fe3O4 hybrid magnetic nano-composite modified glassy carbon electrode for tryptophan sensing. Sensors and Actuators B: Chemical, 2012, 163, 171-178.	4.0	92
25	Red-green-blue fluorescent hollow carbon nanoparticles isolated from chromatographic fractions for cellular imaging. Nanoscale, 2014, 6, 8162.	2.8	89
26	Real-Time Monitoring Mitochondrial Viscosity during Mitophagy Using a Mitochondria-Immobilized Near-Infrared Aggregation-Induced Emission Probe. Analytical Chemistry, 2021, 93, 3241-3249.	3.2	87
27	Facile Synthesis of N-Doped Carbon Dots as a New Matrix for Detection of Hydroxy-Polycyclic Aromatic Hydrocarbons by Negative-Ion Matrix-Assisted Laser Desorption/Ionization Time-of-Flight Mass Spectrometry. ACS Applied Materials & Interfaces, 2016, 8, 12976-12984.	4.0	86
28	Pollution characteristics of ambient PM2.5-bound PAHs and NPAHs in a typical winter time period in Taiyuan. Chinese Chemical Letters, 2014, 25, 663-666.	4.8	84
29	Copper doped carbon dots as the multi-functional fluorescent sensing platform for tetracyclines and pH. Sensors and Actuators B: Chemical, 2021, 330, 129360.	4.0	84
30	An exonuclease I-based label-free fluorometric aptasensor for adenosine triphosphate (ATP) detection with a wide concentration range. Biosensors and Bioelectronics, 2015, 63, 311-316.	5.3	83
31	Carbon dots with red emission as a fluorescent and colorimeteric dual-readout probe for the detection of chromium(<scp>vi</scp>) and cysteine and its logic gate operation. Journal of Materials Chemistry B, 2018, 6, 6099-6107.	2.9	83
32	Electrochemical detection of chloramphenicol using palladium nanoparticles decorated reduced graphene oxide. Microchemical Journal, 2019, 148, 774-783.	2.3	83
33	Highly luminescent N-doped carbon dots from black soya beans for free radical scavenging, Fe3+ sensing and cellular imaging. Spectrochimica Acta - Part A: Molecular and Biomolecular Spectroscopy, 2019, 211, 363-372.	2.0	82
34	Novel far-visible and near-infrared pH probes based on styrylcyanine for imaging intracellular pH in live cells. Chemical Communications, 2012, 48, 11202.	2.2	81
35	Facile and eco-friendly synthesis of green fluorescent carbon nanodots for applications in bioimaging, patterning and staining. Nanoscale, 2015, 7, 7394-7401.	2.8	81
36	A novel far-visible and near-infrared pH probe for monitoring near-neutral physiological pH changes: imaging in live cells. Journal of Materials Chemistry B, 2013, 1, 4281.	2.9	80

#	Article	IF	CITATIONS
37	Application of HPLC and MALDI-TOF MS for Studying As-Synthesized Ligand-Protected Gold Nanoclusters Products. Analytical Chemistry, 2009, 81, 1676-1685.	3.2	79
38	Facile preparation of bright orange fluorescent carbon dots and the constructed biosensing platform for the detection of pH in living cells. Talanta, 2018, 189, 8-15.	2.9	79
39	Red fluorescent carbon dots for tetracycline antibiotics and pH discrimination from aggregation-induced emission mechanism. Sensors and Actuators B: Chemical, 2021, 332, 129513.	4.0	79
40	Nitrogen and phosphorus dual-doped carbon dots as a label-free sensor for Curcumin determination in real sample and cellular imaging. Talanta, 2018, 183, 61-69.	2.9	77
41	Green and facile synthesis of nitrogen-doped carbon nanodots for multicolor cellular imaging and Co2+ sensing in living cells. Sensors and Actuators B: Chemical, 2016, 235, 179-187.	4.0	76
42	3D graphene/hydroxypropyl-β-cyclodextrin nanocomposite as an electrochemical chiral sensor for the recognition of tryptophan enantiomers. Journal of Materials Chemistry C, 2018, 6, 12822-12829.	2.7	76
43	A lysosome-targeting and polarity-specific fluorescent probe for cancer diagnosis. Chemical Communications, 2019, 55, 4703-4706.	2.2	76
44	Green synthesis of carbon nanodots from cotton for multicolor imaging, patterning, and sensing. Sensors and Actuators B: Chemical, 2015, 221, 769-776.	4.0	74
45	Visibleâ€Lightâ€Excited Ultralongâ€Lifetime Room Temperature Phosphorescence Based on Nitrogenâ€Doped Carbon Dots for Double Anticounterfeiting. Advanced Optical Materials, 2020, 8, 1901557.	3.6	71
46	One step hydrothermal synthesis of carbon nanodots to realize the fluorescence detection of picric acid in real samples. Sensors and Actuators B: Chemical, 2018, 258, 580-588.	4.0	70
47	Matrix-Free and Highly Efficient Room-Temperature Phosphorescence of Nitrogen-Doped Carbon Dots. Langmuir, 2018, 34, 12845-12852.	1.6	69
48	Lysozyme-stabilized gold nanoclusters as a novel fluorescence probe for cyanide recognition. Spectrochimica Acta - Part A: Molecular and Biomolecular Spectroscopy, 2014, 121, 77-80.	2.0	68
49	High-quality water-soluble luminescent carbon dots for multicolor patterning, sensors, and bioimaging. RSC Advances, 2015, 5, 16972-16979.	1.7	68
50	Facile, rapid synthesis of N,P-dual-doped carbon dots as a label-free multifunctional nanosensor for Mn(VII) detection, temperature sensing and cellular imaging. Sensors and Actuators B: Chemical, 2018, 277, 492-501.	4.0	67
51	Excitation-independent yellow-fluorescent nitrogen-doped carbon nanodots for biological imaging and paper-based sensing. Sensors and Actuators B: Chemical, 2017, 251, 234-241.	4.0	66
52	FRET-based modified graphene quantum dots for direct trypsin quantification in urine. Analytica Chimica Acta, 2016, 917, 64-70.	2.6	64
53	S-Nitrosothiols: chemistry and reactions. Chemical Communications, 2017, 53, 11266-11277.	2.2	63
54	Porphyrin functionalized graphene nanosheets-based electrochemical aptasensor for label-free ATP detection. Journal of Materials Chemistry, 2012, 22, 23900.	6.7	62

#	Article	IF	CITATIONS
55	<i>p</i> -Phenylenediamine Antioxidants in PM _{2.5} : The Underestimated Urban Air Pollutants. Environmental Science & Technology, 2022, 56, 6914-6921.	4.6	61
56	A simple Schiff base fluorescence probe for highly sensitive and selective detection of Hg2+and Cu2+. Talanta, 2016, 154, 278-283.	2.9	60
57	Orange-emitting N-doped carbon dots as fluorescent and colorimetric dual-mode probes for nitrite detection and cellular imaging. Journal of Materials Chemistry B, 2020, 8, 2123-2127.	2.9	59
58	Nitrogen-doped carbon dots as fluorescent probe for detection of curcumin based on the inner filter effect. RSC Advances, 2015, 5, 95054-95060.	1.7	57
59	β-Cyclodextrin functionalized Mn-doped ZnS quantum dots for the chiral sensing of tryptophan enantiomers. Polymer Chemistry, 2015, 6, 591-598.	1.9	57
60	β-Cyclodextrin–Hyaluronic Acid Polymer Functionalized Magnetic Graphene Oxide Nanocomposites for Targeted Photo-Chemotherapy of Tumor Cells. Polymers, 2019, 11, 133.	2.0	57
61	An indole-carbazole-based ratiometric emission pH fluorescent probe for imaging extreme acidity. Sensors and Actuators B: Chemical, 2015, 221, 1069-1076.	4.0	53
62	Synthesis and Characterization of <i>n</i> -Alkylamine-Stabilized Palladium Nanoparticles for Electrochemical Oxidation of Methane. Journal of Physical Chemistry C, 2010, 114, 723-733.	1.5	52
63	Colorimetric sensor for cysteine in human urine based on novel gold nanoparticles. Talanta, 2016, 161, 520-527.	2.9	52
64	An anthraquinone-based highly selective colorimetric and fluorometric sensor for sequential detection of Cu ²⁺ and S ^{2â^'} with intracellular application. Journal of Materials Chemistry B, 2017, 5, 8957-8966.	2.9	52
65	Eco-friendly synthesis of nitrogen-doped carbon nanodots from wool for multicolor cell imaging, patterning, and biosensing. Sensors and Actuators B: Chemical, 2016, 235, 316-324.	4.0	51
66	A two-photon ratiometric fluorescent probe for effective monitoring of lysosomal pH in live cells and cancer tissues. Sensors and Actuators B: Chemical, 2018, 262, 913-921.	4.0	51
67	A Golgi-targeted off–on fluorescent probe for real-time monitoring of pH changes <i>in vivo</i> . Chemical Communications, 2019, 55, 6685-6688.	2.2	51
68	A phenolphthalein-based fluorescent probe for the sequential sensing of Al3+ and Fâ^' ions in aqueous medium and live cells. Spectrochimica Acta - Part A: Molecular and Biomolecular Spectroscopy, 2019, 208, 131-139.	2.0	50
69	Novel Processing for Color-Tunable Luminescence Carbon Dots and Their Advantages in Biological Systems. ACS Sustainable Chemistry and Engineering, 2020, 8, 8585-8592.	3.2	49
70	Rational synthesis of graphene–metal coordination polymer composite nanosheet as enhanced materials for electrochemical biosensing. Journal of Materials Chemistry, 2012, 22, 13166.	6.7	48
71	Thiazole-based ratiometric fluorescence pH probe with large Stokes shift for intracellular imaging. Sensors and Actuators B: Chemical, 2016, 233, 566-573.	4.0	48
72	Gold nanoclusters as fluorescent sensors for selective and sensitive hydrogen sulfide detection. Talanta, 2017, 171, 143-151.	2.9	48

#	Article	IF	CITATIONS
73	Simultaneous electrochemical sensing of serotonin, dopamine and ascorbic acid by using a nanocomposite prepared from reduced graphene oxide, Fe3O4 and hydroxypropyl-β-cyclodextrin. Mikrochimica Acta, 2019, 186, 751.	2.5	48
74	Multi-sensing function integrated nitrogen-doped fluorescent carbon dots as the platform toward multi-mode detection and bioimaging. Talanta, 2020, 210, 120653.	2.9	47
75	An efficient turn-on fluorescence biosensor for the detection of glutathione based on FRET between N,S dual-doped carbon dots and gold nanoparticles. Analytical and Bioanalytical Chemistry, 2019, 411, 6687-6695.	1.9	46
76	Ratiometric fluorescent sensors for sequential on-off-on determination of riboflavin, Ag+ and l-cysteine based on NPCl-doped carbon quantum dots. Analytica Chimica Acta, 2021, 1144, 1-13.	2.6	44
77	A colorimetric and ratiometric fluorescent probe for cyanide sensing in aqueous media and live cells. Journal of Materials Chemistry B, 2019, 7, 4620-4629.	2.9	43
78	A two-photon ratiometric fluorescent probe for highly selective sensing of mitochondrial cysteine in live cells. Analyst, The, 2019, 144, 439-447.	1.7	43
79	Dual role of BSA for synthesis of MnO ₂ nanoparticles and their mediated fluorescent turn-on probe for glutathione determination and cancer cell recognition. Analyst, The, 2019, 144, 1988-1994.	1.7	43
80	Carbon-based dots co-doped with nitrogen and sulfur for Cr(<scp>vi</scp>) sensing and bioimaging. RSC Advances, 2016, 6, 28477-28483.	1.7	42
81	Bright-green-emissive nitrogen-doped carbon dots as a nanoprobe for bifunctional sensing, its logic gate operation and cellular imaging. Talanta, 2018, 179, 554-562.	2.9	40
82	Mn-doped ZnS quantum dots with a 3-mercaptopropionic acid assembly as a ratiometric fluorescence probe for the determination of curcumin. RSC Advances, 2015, 5, 21504-21510.	1.7	39
83	Effective adsorption of phenolic pollutants from water using β-cyclodextrin polymer functionalized Fe ₃ O ₄ magnetic nanoparticles. RSC Advances, 2016, 6, 80955-80963.	1.7	39
84	Visual monitoring of the lysosomal pH changes during autophagy with a red-emission fluorescent probe. Journal of Materials Chemistry B, 2020, 8, 1466-1471.	2.9	39
85	Rapid synthesis of multifunctional carbon nanodots as effective antioxidants, antibacterial agents, and quercetin nanoprobes. Talanta, 2020, 206, 120243.	2.9	38
86	Rapid and Specific Imaging of Extracellular Signaling Molecule Adenosine Triphosphate with a Self-Phosphorylating DNAzyme. Journal of the American Chemical Society, 2021, 143, 15084-15090.	6.6	38
87	Graphene quantum dots wrapped square-plate-like MnO2 nanocomposite as a fluorescent turn-on sensor for glutathione. Talanta, 2020, 219, 121180.	2.9	38
88	Intelligently design primary aromatic amines derived carbon dots for optical dual-mode and smartphone imaging detection of nitrite based on specific diazo coupling. Journal of Hazardous Materials, 2022, 430, 128393.	6.5	38
89	Determination of protein, fat, starch, and amino acids in foxtail millet [Setaria italica (L.) Beauv.] by Fourier transform near-infrared reflectance spectroscopy. Food Science and Biotechnology, 2013, 22, 1495-1500.	1.2	37
90	Label-free aptasensor for thrombin using a glassy carbon electrode modified with a graphene-porphyrin composite. Mikrochimica Acta, 2014, 181, 189-196.	2.5	37

#	Article	IF	CITATIONS
91	β-Cyclodextrin modified graphene oxide–magnetic nanocomposite for targeted delivery and pH-sensitive release of stereoisomeric anti-cancer drugs. RSC Advances, 2015, 5, 89299-89308.	1.7	36
92	Facile synthesis of iron phthalocyanine functionalized N,B–doped reduced graphene oxide nanocomposites and sensitive electrochemical detection for glutathione. Sensors and Actuators B: Chemical, 2019, 297, 126756.	4.0	36
93	Fe3+ and intracellular pH determination based on orange fluorescence carbon dots co-doped with boron, nitrogen and sulfur. Materials Science and Engineering C, 2021, 118, 111478.	3.8	36
94	Facile synthesis of multifunctional carbon dots with 54.4% orange emission for label-free detection of morin and endogenous/exogenous hypochlorite. Journal of Hazardous Materials, 2022, 424, 127289.	6.5	36
95	Beyond Substituted <i>p</i> -Phenylenediamine Antioxidants: Prevalence of Their Quinone Derivatives in PM _{2.5} . Environmental Science & Technology, 2022, 56, 10629-10637.	4.6	36
96	One-step synthesis of a dual-emitting carbon dot-based ratiometric fluorescent probe for the visual assay of Pb ²⁺ and PPi and development of a paper sensor. Journal of Materials Chemistry B, 2019, 7, 5502-5509.	2.9	35
97	Construction of CPs@MnO ₂ –AgNPs as a multifunctional nanosensor for glutathione sensing and cancer theranostics. Nanoscale, 2019, 11, 18845-18853.	2.8	35
98	Facile synthesis of ratiometric fluorescent carbon dots for pH visual sensing and cellular imaging. Talanta, 2020, 216, 120943.	2.9	35
99	Visible-light-driven photoelectrochemical sensing platform based on BiOI nanoflowers/TiO2 nanotubes for detection of atrazine in environmental samples. Journal of Hazardous Materials, 2021, 409, 124894.	6.5	35
100	Colorimetric detection of riboflavin by silver nanoparticles capped with β-cyclodextrin-grafted citrate. Colloids and Surfaces B: Biointerfaces, 2016, 148, 66-72.	2.5	34
101	Comparative study of Cl,N-Cdots and N-Cdots and application for trinitrophenol and ClOâ^' sensor and cell-imaging. Analytica Chimica Acta, 2019, 1091, 76-87.	2.6	34
102	A highly efficient chiral sensing platform for tryptophan isomers based on a coordination self-assembly. Talanta, 2019, 195, 306-312.	2.9	34
103	An anthraquinone-imidazole-based colorimetric and fluorescent sensor for the sequential detection of Ag ⁺ and biothiols in living cells. Analyst, The, 2020, 145, 3029-3037.	1.7	34
104	A <scp>Mitochondriaâ€Specific</scp> Orange/ <scp>Nearâ€Infraredâ€Emissive</scp> Fluorescent Probe for <scp>Dualâ€Imaging</scp> of Viscosity and <scp>H₂O₂</scp> in Inflammation and Tumor Models. Chinese Journal of Chemistry, 2021, 39, 1303-1309.	2.6	34
105	High-performance liquid chromatographic and mass spectrometric analysis of fluorescent carbon nanodots. Talanta, 2014, 129, 529-538.	2.9	33
106	Label-free and highly selective electrochemical aptasensor for detection of PCBs based on nickel hexacyanoferrate nanoparticles/reduced graphene oxides hybrids. Biosensors and Bioelectronics, 2019, 145, 111728.	5.3	33
107	A label-free nano-probe for sequential and quantitative determination of Cr(VI) and ascorbic acid in real samples based on S and N dual-doped carbon dots. Spectrochimica Acta - Part A: Molecular and Biomolecular Spectroscopy, 2019, 215, 58-68.	2.0	33
108	Electrocatalytic oxidation of formaldehyde and methanol on Ni(OH)2/Ni electrode. Russian Journal of Electrochemistry, 2013, 49, 888-894.	0.3	32

#	Article	IF	CITATIONS
109	A reversible fluorescent pH-sensing system based on the one-pot synthesis of natural silk fibroin-capped copper nanoclusters. Journal of Materials Chemistry C, 2016, 4, 3540-3545.	2.7	32
110	Carbon-supported X-manganate (X Ni, Zn, and Cu) nanocomposites for sensitive electrochemical detection of trace heavy metal ions. Journal of Hazardous Materials, 2022, 435, 129036.	6.5	32
111	Targeted delivery and pH-responsive release of stereoisomeric anti-cancer drugs using β-cyclodextrin assemblied Fe3O4 nanoparticles. Applied Surface Science, 2015, 357, 2077-2086.	3.1	31
112	Development of a Room Temperature SAW Methane Gas Sensor Incorporating a Supramolecular Cryptophane A Coating. Sensors, 2016, 16, 73.	2.1	31
113	A lysozyme-stabilized silver nanocluster fluorescent probe for the detection of sulfide ions. Analytical Methods, 2016, 8, 4328-4333.	1.3	31
114	A naphthalene-based fluorescent probe with a large Stokes shift for mitochondrial pH imaging. Analyst, The, 2018, 143, 5054-5060.	1.7	31
115	Concentration-dependent multicolor fluorescent carbon dots for colorimetric and fluorescent bimodal detections of Fe ³⁺ and <scp>l</scp> -ascorbic acid. Analytical Methods, 2019, 11, 669-676.	1.3	31
116	Design of a facile and label-free electrochemical aptasensor for detection of atrazine. Talanta, 2019, 201, 156-164.	2.9	31
117	A far-red FRET fluorescent probe for ratiometric detection of l-cysteine based on carbon dots and N-acetyl-l-cysteine-capped gold nanoparticles. Spectrochimica Acta - Part A: Molecular and Biomolecular Spectroscopy, 2019, 213, 90-96.	2.0	31
118	Label-free fluorescent aptasensor for potassium ion using structure-switching aptamers and berberine. Spectrochimica Acta - Part A: Molecular and Biomolecular Spectroscopy, 2015, 136, 1635-1641.	2.0	29
119	Green-fluorescent nitrogen-doped carbon nanodots for biological imaging and paper-based sensing. Analytical Methods, 2017, 9, 2197-2204.	1.3	29
120	Folate - targeting and bovine serum albumin-gated mesoporous silica nanoparticles as a redox-responsive carrier for epirubicin release. New Journal of Chemistry, 2019, 43, 2694-2701.	1.4	29
121	"On-off-on―detection of Fe3+ and Fâ^', biological imaging, and its logic gate operation based on excitation-independent blue-fluorescent carbon dots. Spectrochimica Acta - Part A: Molecular and Biomolecular Spectroscopy, 2020, 227, 117716.	2.0	29
122	A label-free multifunctional nanosensor based on N-doped carbon nanodots for vitamin B ₁₂ and Co ²⁺ detection, and bioimaging in living cells and zebrafish. Journal of Materials Chemistry B, 2020, 8, 5089-5095.	2.9	29
123	Azithromycin detection in cells and tablets by N,S co-doped carbon quantum dots. Spectrochimica Acta - Part A: Molecular and Biomolecular Spectroscopy, 2021, 252, 119506.	2.0	29
124	Facile synthesis of orange fluorescence multifunctional carbon dots for label-free detection of vitamin B12 and endogenous/exogenous peroxynitrite. Journal of Hazardous Materials, 2021, 408, 124422.	6.5	28
125	Real-time tracking the mitochondrial membrane potential by a mitochondria-lysosomes migration fluorescent probe with NIR-emissive AIE characteristics. Sensors and Actuators B: Chemical, 2021, 327, 128929.	4.0	28
126	Carbon Nanodots as a Multifunctional Fluorescent Sensing Platform for Ratiometric Determination of Vitamin B ₂ and "Turn-Off―Detection of pH. Journal of Agricultural and Food Chemistry, 2021, 69, 2836-2844.	2.4	28

#	Article	IF	CITATIONS
127	Tricolor emission carbon dots for label-free ratiometric fluorescent and colorimetric recognition of Al3+ and pyrophosphate ion and cellular imaging. Sensors and Actuators B: Chemical, 2021, 345, 130375.	4.0	28
128	Gadolinium-doped carbon dots as a ratiometric fluorometry and colorimetry dual-mode nano-sensor based on specific chelation for morin detection. Sensors and Actuators B: Chemical, 2022, 352, 130991.	4.0	28
129	A selectively fluorescein-based colorimetric probe for detecting copper(II) ion. Spectrochimica Acta - Part A: Molecular and Biomolecular Spectroscopy, 2014, 122, 731-736.	2.0	27
130	A novel fluorescein-based colorimetric probe for Cu ²⁺ detection. RSC Advances, 2016, 6, 59677-59683.	1.7	27
131	Effects of ambient PM _{2.5} and 9-nitroanthracene on DNA damage and repair, oxidative stress and metabolic enzymes in the lungs of rats. Toxicology Research, 2017, 6, 654-663.	0.9	27
132	Synthesis of neutral red covalently functionalized graphene nanocomposite and the electrocatalytic properties toward uric acid. Journal of Materials Chemistry, 2012, 22, 602-608.	6.7	26
133	A selectively rhodamine-based colorimetric probe for detecting copper(II) ion. Spectrochimica Acta - Part A: Molecular and Biomolecular Spectroscopy, 2014, 132, 191-197.	2.0	26
134	Facile Fabrication Route of Janus Gold-Mesoporous Silica Nanocarriers with Dual-Drug Delivery for Tumor Therapy. ACS Biomaterials Science and Engineering, 2020, 6, 1573-1581.	2.6	26
135	Design of long-wavelength emission carbon dots for hypochlorous detection and cellular imaging. Talanta, 2020, 219, 121170.	2.9	26
136	Highly sensitive photoelectrochemical aptasensor based on MoS2 quantum dots/TiO2 nanotubes for detection of atrazine. Sensors and Actuators B: Chemical, 2021, 334, 129652.	4.0	26
137	Recent advances in synthesis and applications of room temperature phosphorescence carbon dots. Talanta, 2021, 231, 122350.	2.9	26
138	A selective carbazole-based fluorescent probe for chromium(iii). Analytical Methods, 2013, 5, 5549.	1.3	25
139	A turn-off-on near-infrared photoluminescence sensor for sequential detection of Fe3+ and ascorbic acid based on glutathione-capped gold nanoclusters. Spectrochimica Acta - Part A: Molecular and Biomolecular Spectroscopy, 2021, 247, 119085.	2.0	25
140	Highly sensitive and selective photoelectrochemical aptasensing of di-2-ethylhexyl phthalate based on graphene quantum dots decorated TiO2 nanotube arrays. Journal of Hazardous Materials, 2022, 426, 128107.	6.5	25
141	Nitrogen-doped carbon dots coupled with morin-Al3+: Cleverly design an integrated sensing platform for ratiometric optical dual-mode and smartphone-assisted visual detection of fluoride ion. Journal of Hazardous Materials, 2022, 439, 129596.	6.5	25
142	Immobilization of platinum nanoparticles and glucose oxidase on eggshell membrane for glucose detection. Analytical Methods, 2013, 5, 5154.	1.3	24
143	Fluorescence enhancement detection of uric acid based on water-soluble 3-mercaptopropionic acid-capped core/shell ZnS:Cu/ZnS. RSC Advances, 2014, 4, 25183-25188.	1.7	24
144	TiO ₂ –graphene hybrid nanostructures by atomic layer deposition with enhanced electrochemical performance for Pb(<scp>ii</scp>) and Cd(<scp>ii</scp>) detection. RSC Advances, 2015, 5, 4343-4349.	1.7	24

#	Article	IF	CITATIONS
145	A colorimetric probe for the detection of aluminum ions based on 11-mercaptoundecanoic acid functionalized gold nanoparticles. Analytical Methods, 2016, 8, 7232-7236.	1.3	24
146	Facile synthesis of ultrahigh fluorescence N,S-self-doped carbon nanodots and their multiple applications for H ₂ S sensing, bioimaging in live cells and zebrafish, and anti-counterfeiting. Nanoscale, 2020, 12, 20482-20490.	2.8	24
147	A fast detection of peroxynitrite in living cells. Analytica Chimica Acta, 2020, 1106, 96-102.	2.6	24
148	Facilely synthesized ultrathin Ni6MnO8@C nanosheets: excellent electrochemical performance and enhanced electrocatalytic epinephrine sensing. Sensors and Actuators B: Chemical, 2021, 326, 128863.	4.0	24
149	A mitochondria-targeted and viscosity-sensitive near-infrared fluorescent probe for visualization of fatty liver, inflammation and photodynamic cancer therapy. Chemical Engineering Journal, 2022, 449, 137762.	6.6	24
150	β-Cyclodextrin derivatives hybrid Fe3O4 magnetic nanoparticles as the drug delivery for ketoprofen. Journal of Inclusion Phenomena and Macrocyclic Chemistry, 2014, 80, 209-215.	0.9	23
151	Carbon quantum dots doped with phosphorus and nitrogen are a viable fluorescent nanoprobe for determination and cellular imaging of vitamin B12 and cobalt(II). Mikrochimica Acta, 2019, 186, 506.	2.5	23
152	Excitation-independent hollow orange-fluorescent carbon nanoparticles for pH sensing in aqueous solution and living cells. Talanta, 2019, 196, 109-116.	2.9	23
153	Novel strategy of electrochemical analysis of DNA bases with enhanced performance based on copperâ~nickel nanosphere decorated N,Bâ~doped reduced graphene oxide. Biosensors and Bioelectronics, 2020, 147, 111735.	5.3	23
154	Monitoring of the decreased mitochondrial viscosity during heat stroke with a mitochondrial AIE probe. Analytical and Bioanalytical Chemistry, 2021, 413, 3823-3831.	1.9	23
155	Down-regulation of aquaporin3 expression by lipopolysaccharide via p38/c-Jun N-terminal kinase signalling pathway in HT-29 human colon epithelial cells. World Journal of Gastroenterology, 2015, 21, 4547-4554.	1.4	22
156	Facile one-pot synthesis of Au(0)@Au(<scp>i</scp>)–NAC core–shell nanoclusters with orange-yellow luminescence for cancer cell imaging. RSC Advances, 2016, 6, 8612-8619.	1.7	22
157	A novel pH fluorescent probe based on indocyanine for imaging of living cells. Dyes and Pigments, 2016, 126, 224-231.	2.0	22
158	A di-functional and label-free carbon-based chem-nanosensor for real-time monitoring of pH fluctuation and quantitative determining of Curcumin. Analytica Chimica Acta, 2019, 1057, 132-144.	2.6	22
159	The ratiometric fluorescent probe with high quantum yield for quantitative imaging of intracellular pH. Talanta, 2020, 208, 120279.	2.9	22
160	Highly sensitive fluorescent carbon dots probe with ratiometric emission for the determination of ClO ^{â^'} . Analyst, The, 2020, 145, 2212-2218.	1.7	22
161	One-step synthesis of red emission multifunctional carbon dots for label-free detection of berberine and curcumin and cell imaging. Spectrochimica Acta - Part A: Molecular and Biomolecular Spectroscopy, 2021, 251, 119432.	2.0	22
162	Carbon dots for ratiometric fluorescence detection of morin. Spectrochimica Acta - Part A: Molecular and Biomolecular Spectroscopy, 2021, 256, 119751.	2.0	22

#	Article	IF	CITATIONS
163	Enzyme free glucose sensing by amino-functionalized silicon quantum dot. Spectrochimica Acta - Part A: Molecular and Biomolecular Spectroscopy, 2019, 216, 303-309.	2.0	21
164	Highly efficient removal of cationic, anionic and neutral dyes by hierarchically porous structured three-dimensional magnetic sulfur/nitrogen co-doped reduced graphene oxide nanohybrid. Journal of Water Process Engineering, 2020, 37, 101345.	2.6	21
165	Fe ³⁺ detection, bioimaging, and patterning based on bright blue-fluorescent N-doped carbon dots. Analyst, The, 2020, 145, 5450-5457.	1.7	21
166	Tumor microenvironment responsive mesoporous silica nanoparticles for dual delivery of doxorubicin and chemodynamic therapy (CDT) agent. New Journal of Chemistry, 2020, 44, 2578-2586.	1.4	21
167	A strategy of electrochemical simultaneous detection of acetaminophen and levofloxacin in water based on g-C ₃ N ₄ nanosheet-doped graphene oxide. Environmental Science: Nano, 2021, 8, 258-268.	2.2	21
168	11-Mercaptoundecanoic Acid-Functionalized Carbon Dots As a Ratiometric Optical Probe for Doxorubicin Detection. ACS Applied Nano Materials, 2021, 4, 13734-13746.	2.4	21
169	Quantitative analysis of nitro-polycyclic aromatic hydrocarbons in PM _{2.5} samples with graphene as a matrix by MALDI-TOF MS. Analytical Methods, 2015, 7, 3967-3971.	1.3	20
170	Schisandrin B inhibits Th1/Th17 differentiation and promotes regulatory T cell expansion in mouse lymphocytes. International Immunopharmacology, 2016, 35, 257-264.	1.7	20
171	Effects of sub-chronic exposure to atmospheric PM _{2.5} on fibrosis, inflammation, endoplasmic reticulum stress and apoptosis in the livers of rats. Toxicology Research, 2018, 7, 271-282.	0.9	20
172	Planar Pentacoordinate versus Tetracoordinate Carbons in Ternary CBe ₄ Li ₄ and CBe ₄ Li ₄ ^{2–} Clusters. Journal of Physical Chemistry A, 2018, 122, 8370-8376.	1.1	20
173	Recent Advances in Carbon Nanodots: Properties and Applications in Cancer Diagnosis and Treatment. Journal of Analysis and Testing, 2019, 3, 37-49.	2.5	20
174	The design of hydrogen sulfide fluorescence probe based on dual nucleophilic reaction and its application for bioimaging. Spectrochimica Acta - Part A: Molecular and Biomolecular Spectroscopy, 2019, 207, 150-155.	2.0	20
175	Silk Fibroin-Confined Star-Shaped Decahedral Silver Nanoparticles as Fluorescent Probe for Detection of Cu ²⁺ and Pyrophosphate. ACS Biomaterials Science and Engineering, 2020, 6, 2770-2777.	2.6	20
176	Nitrogen-doped carbon dots for wash-free imaging of nucleolus orientation. Mikrochimica Acta, 2021, 188, 183.	2.5	20
177	Synthesis of a Palladium-Graphene Material and Its Application for Formaldehyde Determination. Analytical Letters, 2013, 46, 1454-1465.	1.0	19
178	A highly selective ratiometric fluorescent probe for biothiol and imaging in live cells. RSC Advances, 2016, 6, 43028-43033.	1.7	19
179	A lysosome-targetable fluorescent probe for real-time imaging cysteine under oxidative stress in living cells. Spectrochimica Acta - Part A: Molecular and Biomolecular Spectroscopy, 2019, 221, 117175.	2.0	19
180	A ratiometric and far-red fluorescence "off-on―sensor for sequential determination of copper(II) and L-histidine based on FRET system between N-acetyl-L-cysteine-capped AuNCs and N,S,P co-doped carbon dots. Mikrochimica Acta, 2020, 187, 299.	2.5	19

#	Article	IF	CITATIONS
181	A one-pot synthesis of fluorescent N,P-codoped carbon dots for vitamin B ₁₂ determination and bioimaging application. New Journal of Chemistry, 2021, 45, 3508-3514.	1.4	19
182	Electrochemical Behavior of Hydrogen Peroxide at a Glassy Carbon Electrode Modified with Nickel Hydroxide–Decorated Multiwalled Carbon Nanotubes. Analytical Letters, 2008, 41, 3147-3160.	1.0	18
183	UHPLC combined with mass spectrometric study of as-synthesized carbon dots samples. Talanta, 2016, 146, 340-350.	2.9	18
184	One-pot synthesis of aqueous soluble and organic soluble carbon dots and their multi-functional applications. Talanta, 2019, 202, 375-383.	2.9	18
185	An "on–off–on―fluorescent nanoprobe for recognition of Cu ²⁺ and GSH based on nitrogen co-doped carbon quantum dots, and its logic gate operation. Analytical Methods, 2019, 11, 2650-2657.	1.3	18
186	Effects of Ambient Atmospheric PM2.5, 1-Nitropyrene and 9-Nitroanthracene on DNA Damage and Oxidative Stress in Hearts of Rats. Cardiovascular Toxicology, 2019, 19, 178-190.	1.1	18
187	Discovery of emerging sulfur-containing PAHs in PM2.5: Contamination profiles and potential health risks. Journal of Hazardous Materials, 2021, 416, 125795.	6.5	18
188	A facile synthesis of long-wavelength emission nitrogen-doped carbon dots for intracellular pH variation and hypochlorite sensing. Biomaterials Science, 2021, 9, 2255-2261.	2.6	18
189	Rapid one-pot synthesis of MMTA protected fluorescent gold nanoclusters for selective and sensitive detection of ferric ion. Talanta, 2017, 174, 44-51.	2.9	17
190	Ternary 12-electron CBe ₃ X ₃ ⁺ (X = H, Li, Na, Cu, Ag) clusters: planar tetracoordinate carbons and superalkali cations. Physical Chemistry Chemical Physics, 2019, 21, 22048-22056.	1.3	17
191	A turn-on fluorescence probe for cysteine/homocysteine based on the nucleophilic-induced rearrangement of benzothiazole thioether. Spectrochimica Acta - Part A: Molecular and Biomolecular Spectroscopy, 2019, 222, 117262.	2.0	17
192	Hypoxia imaging in living cells, tissues and zebrafish with a nitroreductase-specific fluorescent probe. Analyst, The, 2020, 145, 5657-5663.	1.7	17
193	A turn-on fluorescence probe for hydrogen sulfide in absolute aqueous solution. Spectrochimica Acta - Part A: Molecular and Biomolecular Spectroscopy, 2020, 233, 118156.	2.0	17
194	N-Doped carbon dots for the fluorescence and colorimetry dual-mode detection of curcumin. Analyst, The, 2021, 146, 5357-5361.	1.7	17
195	Stimuli-Responsive Three-Dimensional DNA Nanomachines Engineered by Controlling Dynamic Interactions at Biomolecule-Nanoparticle Interfaces. ACS Nano, 2021, 15, 16870-16877.	7.3	17
196	Three birds with one stone: a single AlEgen for dual-organelle imaging, cell viability evaluation and photodynamic cancer cell ablation. Materials Chemistry Frontiers, 2022, 6, 333-340.	3.2	17
197	Dendritic Mesoporous Silica Nanoparticle-Tuned High-Affinity MnO ₂ Nanozyme for Multisignal GSH Sensing and Target Cancer Cell Detection. ACS Sustainable Chemistry and Engineering, 2022, 10, 5911-5921.	3.2	17
198	Fluorescence Quenching of Pheophytin-a by Copper(II) Ions. Chinese Journal of Chemistry, 2009, 27, 513-517.	2.6	16

#	Article	IF	CITATIONS
199	<i>β</i> yclodextrin and Its Derivatives Functionalized Magnetic Nanoparticles for Targeting Delivery of Curcumin and Cell Imaging. Chinese Journal of Chemistry, 2016, 34, 599-608.	2.6	16
200	A highly selective fluorescent probe based on Michael addition for fast detection of hydrogen sulfide. Spectrochimica Acta - Part A: Molecular and Biomolecular Spectroscopy, 2017, 173, 457-461.	2.0	16
201	A red-emission fluorescent probe for visual monitoring of lysosomal pH changes during mitophagy and cell apoptosis. Analyst, The, 2020, 145, 7018-7024.	1.7	16
202	Nitrogen, sulfur, phosphorus, and chlorine co-doped carbon nanodots as an "off-on―fluorescent probe for sequential detection of curcumin and europium ion and luxuriant applications. Mikrochimica Acta, 2021, 188, 16.	2.5	16
203	Biodegradable Fluorescent SiO ₂ @MnO ₂ -Based Sequence Strategy for Glutathione Sensing in a Biological System and Synergistic Theragnostics to Cancer Cells. ACS Sustainable Chemistry and Engineering, 2021, 9, 2770-2783.	3.2	16
204	Development of a piperazinyl-NBD-based fluorescent probe and its dual-channel detection for hydrogen sulfide. Analyst, The, 2021, 146, 2138-2143.	1.7	16
205	Dicyanoisophorone-based fluorescent probe with large Stokes shift for ratiometric detection and imaging of exogenous/endogenous hypochlorite in cell and zebrafish. Talanta, 2022, 242, 123293.	2.9	16
206	Co ²⁺ detection, cell imaging, and temperature sensing based on excitation-independent green-fluorescent N-doped carbon dots. RSC Advances, 2019, 9, 41361-41367.	1.7	15
207	Biosensors for Determination of Galactose with Galactose Oxidase Immobilized on Eggshell Membrane. Analytical Letters, 2005, 38, 1519-1529.	1.0	14
208	A novel asymmetric indolo[3,2-b]carbazole derivative containing benzothiazole and dimesitylboron units: Synthesis, photophysical and sensing properties. Synthetic Metals, 2013, 179, 42-48.	2.1	14
209	Enhanced Sensitivity of a Love Wave-Based Methane Gas Sensor Incorporating a Cryptophane-A Thin Film. Sensors, 2018, 18, 3247.	2.1	14
210	Dual-ligand functionalized carbon nanodots as green fluorescent nanosensors for cellular dual receptor-mediated targeted imaging. Analyst, The, 2019, 144, 6729-6735.	1.7	14
211	Gold nanoparticles decorated bimetallic CuNi-based hollow nanoarchitecture for theÂenhancement ofÂelectrochemical sensing performance of nitrite. Mikrochimica Acta, 2020, 187, 572.	2.5	14
212	Smilax China-derived yellow-fluorescent carbon dots for temperature sensing, Cu ²⁺ detection and cell imaging. Analyst, The, 2020, 145, 2176-2183.	1.7	14
213	MnO ₂ nanosheets anchored with polypyrrole nanoparticles as a multifunctional platform for combined photothermal/photodynamic therapy of tumors. Food and Function, 2021, 12, 6334-6347.	2.1	14
214	A bifunctional fluorescence probe for dual-channel detecting of mitochondrial viscosity and endogenous/exogenous peroxynitrite. Bioorganic Chemistry, 2022, 119, 105484.	2.0	14
215	Preparation of yellow-emitting carbon dots and their bifunctional detection of tetracyclines and Al3+ in food and living cells. Mikrochimica Acta, 2021, 188, 418.	2.5	14
216	Spectroscopic studies on the inclusion interaction of p-sulfonatocalix[6]arene with vitamin B6. Journal of Inclusion Phenomena and Macrocyclic Chemistry, 2012, 72, 389-395.	1.6	13

#	Article	IF	CITATIONS
217	Changes in nutritional constituents, anthocyanins, and volatile compounds during the processing of black rice tea. Food Science and Biotechnology, 2013, 22, 917-923.	1.2	13
218	A benzimidazole-based highly selective colorimetric and far-red fluorometric pH sensor for intracellular imaging. New Journal of Chemistry, 2018, 42, 12954-12959.	1.4	13
219	Sulforaphane-Conjugated Carbon Dots: A Versatile Nanosystem for Targeted Imaging and Inhibition of EGFR-Overexpressing Cancer Cells. ACS Biomaterials Science and Engineering, 2019, 5, 4692-4699.	2.6	13
220	Novel long-wavelength emissive lysosome-targeting ratiometric fluorescent probes for imaging in live cells. Analyst, The, 2019, 144, 4288-4294.	1.7	13
221	Boronate based sensitive fluorescent probe for the detection of endogenous peroxynitrite in living cells. Spectrochimica Acta - Part A: Molecular and Biomolecular Spectroscopy, 2020, 243, 118683.	2.0	13
222	N, Cl-doped carbon dots for fluorescence and colorimetric dual-mode detection of water in tetrahydrofuran and development of aApaper-based sensor. Mikrochimica Acta, 2021, 188, 324.	2.5	13
223	Imaging of lysosomal pH changes with a novel quinoline/benzothiazole probe. New Journal of Chemistry, 2018, 42, 13479-13485.	1.4	12
224	Dual sensing reporter system of assembled gold nanoparticles toward the sequential colorimetric detection of adenosine and Cr(III). Talanta, 2019, 204, 294-303.	2.9	12
225	A benzothiazolium-based fluorescent probe with ideal p <i>K</i> _a for mitochondrial pH imaging and cancer cell differentiation. Journal of Materials Chemistry B, 2020, 8, 10586-10592.	2.9	12
226	Convenient synthesis of carbon nanodots for detecting Cr(<scp>vi</scp>) and ascorbic acid by fluorimetry. New Journal of Chemistry, 2020, 44, 20806-20811.	1.4	12
227	Enhanced chemical sensing for Cu ²⁺ based on composites of ZIF-8 with small molecules. RSC Advances, 2020, 10, 13998-14006.	1.7	12
228	Synthesis of carbon dots for Al ³⁺ sensing in water by fluorescence assay. Luminescence, 2021, 36, 1469-1475.	1.5	12
229	A highly sensitive photoelectrochemical aptasensor based on BiVO4 nanoparticles-TiO2 nanotubes for detection of PCB72. Talanta, 2021, 233, 122551.	2.9	12
230	Orange emissive carbon nanodots for fluorescent and colorimetric bimodal discrimination of Cu ²⁺ and pH. Analyst, The, 2021, 146, 1907-1914.	1.7	12
231	Sensitive and selective detection of l-tryptophan using Mn–ZnS QDs as the ratiometric emission probe. Analytical Methods, 2014, 6, 3227.	1.3	11
232	Indole-based pH probe with ratiometric fluorescence behavior for intracellular imaging. RSC Advances, 2015, 5, 99739-99744.	1.7	11
233	Amperometric Biosensor for Detection of Phenolic Compounds Based on Tyrosinase, <i>N</i> â€Acetylâ€ <i>L</i> â€cysteineâ€capped Gold Nanoparticles and Chitosan Nanocomposite. Chinese Journal of Chemistry, 2017, 35, 1305-1310.	2.6	11
234	A butterfly-shaped ESIPT molecule with solid-state fluorescence for the detection of latent fingerprints and exogenous and endogenous ONOOâ^' by caging of the phenol donor. Talanta, 2021, 233, 122593.	2.9	11

#	Article	IF	CITATIONS
235	AIE-based fluorescent boronate probe and its application in peroxynitrite imaging. Spectrochimica Acta - Part A: Molecular and Biomolecular Spectroscopy, 2021, 261, 120044.	2.0	11
236	A novel phenolphthalein-based fluorescent chemosensor for pyrophosphate detection via an Al3+ displacement approach in real samples and living cells. Spectrochimica Acta - Part A: Molecular and Biomolecular Spectroscopy, 2022, 276, 121174.	2.0	11
237	Three-Dimensional Flower-like Nickel Oxide/Graphene Nanostructures for Electrochemical Detection of Environmental Nitrite. ACS Applied Nano Materials, 2022, 5, 216-226.	2.4	11
238	Piperazine-Based Mitochondria-Immobilized pH Fluorescent Probe for Imaging Endogenous ONOO [–] and Real-Time Tracking of Mitophagy. ACS Applied Bio Materials, 2022, 5, 2777-2785.	2.3	11
239	Electrocatalytic oxidation of formaldehyde and formic acid at Pd nanoparticles modified glassy carbon electrode. Micro and Nano Letters, 2013, 8, 704-708.	0.6	10
240	High-performance liquid chromatography coupled with mass spectrometry for analysis of ultrasmall palladium nanoparticles. Talanta, 2015, 131, 632-639.	2.9	10
241	Determination of Mercury(II) by Fluorescence Using Deoxyribonucleic Acid Stabilized Silver Nanoclusters. Analytical Letters, 2015, 48, 281-290.	1.0	10
242	A fluorometric and colorimetric dual-readout nanoprobe based on Cl and N co-doped carbon quantum dots with large stokes shift for sequential detection of morin and zinc ion. Spectrochimica Acta - Part A: Molecular and Biomolecular Spectroscopy, 2021, 261, 120028.	2.0	10
243	A selective electrochemical chiral interface based on a carboxymethyl-β-cyclodextrin/Pd@Au nanoparticles/3D reduced graphene oxide nanocomposite for tyrosine enantiomer recognition. Analyst, The, 2022, 147, 880-888.	1.7	10
244	Electro-Oxidation of Methane on Roughened Palladium Electrode in Acidic Electrolytes at Ambient Temperatures. Analytical Letters, 2010, 43, 1055-1065.	1.0	9
245	β-Cyclodextrin functionalized gold nanoparticles: characterization and its analytical application for l-tyrosine. Journal of Inclusion Phenomena and Macrocyclic Chemistry, 2014, 78, 275-286.	0.9	9
246	Green Synthesis of Gold Nanoparticles with Pectinase: a Highly Selective and Ultra-Sensitive Colorimetric Assay for Mg2+. Plasmonics, 2017, 12, 717-727.	1.8	9
247	A designer 32-electron superatomic CBe8H12 cluster: core–shell geometry, octacoordinate carbon, and cubic aromaticity. New Journal of Chemistry, 2020, 44, 7286-7292.	1.4	9
248	TICT-Based Microenvironment-Sensitive Probe with Turn-on Red Emission for Human Serum Albumin Detection and for Targeting Lipid Droplet Imaging. ACS Biomaterials Science and Engineering, 2022, 8, 253-260.	2.6	9
249	A specific discriminating GSH from Cys/Hcy fluorescence nanosensor: The carbon dots-MnO2 nanocomposites. Sensors and Actuators B: Chemical, 2022, 367, 132135.	4.0	9
250	The Interaction of Piroxicam with Neutral (HP-β-CD) and Anionically Charged (SBE-β-CD) β-cyclodextrin. Journal of Inclusion Phenomena and Macrocyclic Chemistry, 2006, 56, 215-220.	1.6	8
251	Voltammetric Study and Detection of Methane on Nickel Hydroxide–Modified Nickel Electrode. Analytical Letters, 2008, 41, 593-598.	1.0	8
252	β-Amyloid Biomarker Detection for Alzheimer's Disease. Journal of Analysis and Testing, 2017, 1, 1.	2.5	8

#	Article	IF	CITATIONS
253	Controllable Fabrication, Photoluminescence Mechanism, and Novel Application of Green–Yellow–Orange Fluorescent Carbon-Based Nanodots. ACS Biomaterials Science and Engineering, 2019, 5, 5060-5071.	2.6	8
254	Real-world PM2.5 exposure induces pathological injury and DNA damage associated with miRNAs and DNA methylation alteration in rat lungs. Environmental Science and Pollution Research, 2022, 29, 28788-28803.	2.7	8
255	A lipid droplet-targetable and biothiol-sensitive fluorescent probe for the diagnosis of cancer cells/tissues. Analyst, The, 2022, 147, 1695-1701.	1.7	8
256	STUDY ON THE PAPER SUBSTRATE ROOM TEMPERATURE PHOSPHORESCENCE OF CRYPTOTANSHINONE AND TANSHINONE IIA USING FILTER PAPER AS SUBSTRATE AND ANALYTICAL APPLICATION. Analytical Letters, 2002, 35, 2319-2330.	1.0	7
257	Study on the intermolecular complexation behavior between p-sulfonatocalix[4]arene with l-tyrosine. Journal of Inclusion Phenomena and Macrocyclic Chemistry, 2012, 72, 473-479.	1.6	7
258	Magnetic solid-phase extraction based on a trimethylstearylammonium bromide coated Fe3O4/SiO2 composite for determination of adriamycin hydrochloride in human plasma and urine by HPLC-FLD. Analytical Methods, 2014, 6, 6736-6744.	1.3	7
259	Chromatographic separation and mass spectrometric analysis of N-acetyl- <scp>I</scp> -cysteine-protected palladium nanoparticles. Analytical Methods, 2017, 9, 4539-4546.	1.3	7
260	Reduced carbon nanodots as a novel substrate for direct analysis of bisphenol analogs in surface assisted laser desorption/ionization time of flight mass spectrometry. Talanta, 2018, 190, 89-94.	2.9	7
261	An efficient fluorescent nano-sensor of N-doped carbon dots for the determination of 2,4,6-trinitrophenol and other applications. Analytical Methods, 2020, 12, 5195-5201.	1.3	7
262	Gold/Palladium–Polypyrrole/Graphene Nanocomposites for Simultaneous Electrochemical Detection of DNA Bases. ACS Applied Nano Materials, 2022, 5, 1635-1643.	2.4	7
263	l-Ascorbic acid biosensing assay from enzyme-immobilized pig bladder membrane as a novel platform. Analytical Methods, 2013, 5, 1253.	1.3	6
264	Fiber-Optic Sucrose Sensor Based on Mode-Filtered Light Detection. Journal of Carbohydrate Chemistry, 2013, 32, 475-482.	0.4	6
265	Substituent Effect on the Properties of pH Fluorescence Probes Containing Pyridine Group. ChemistrySelect, 2019, 4, 5735-5739.	0.7	6
266	Alizarin-based molecular probes for the detection of hydrogen peroxide and peroxynitrite. Analyst, The, 2021, 146, 509-514.	1.7	6
267	Isolation of a Methylobacterium organophilium strain, and its application to a methanol biosensor. Mikrochimica Acta, 2009, 167, 67-73.	2.5	4
268	Study on the inclusion interaction of ethyl violet with cyclodextrins by MWNTs/Nafion modified glassy carbon electrode. Journal of Inclusion Phenomena and Macrocyclic Chemistry, 2010, 68, 467-473.	1.6	4
269	Lysosome targeting, Cr(<scp>vi</scp>) and <scp>l</scp> -AA sensing, and cell imaging based on N-doped blue-fluorescence carbon dots. Analytical Methods, 2021, 13, 3561-3568.	1.3	4
270	An ultrasensitive MnO2-S,O-doped g-C3N4 nanoprobe for "turn-on―detection of glutathione and cell imaging. Journal of Materials Science, 2022, 57, 7909.	1.7	4

#	ARTICLE	IF	CITATIONS
271	Determination of glucose in human serum based on an onion primary cuticula biosensor immobilized glucose oxidase. Analytical Methods, 2012, 4, 1432.	1.3	3
272	Controlled Release of Curcumin via Folic Acid Conjugated Magnetic Drug Delivery System. Chemical Research in Chinese Universities, 2018, 34, 203-211.	1.3	3
273	A waterâ€soluble 1,8â€naphthalimideâ€based fluorescent pH probe for distinguishing tumorous tissues and inflammation in mice. Luminescence, 2022, 37, 1395-1403.	1.5	3
274	An Analytical Application of Ofloxacin by Solid‧ubstrate Room Temperature Phosphorescence. Analytical Letters, 2004, 37, 307-320.	1.0	2
275	Investigation on the Luminescence Performance of Four Quinolones. Analytical Letters, 2006, 39, 603-617.	1.0	2
276	The Solid Surface Room Temperature Phosphorescence of Three Purine Compounds and Analytical Application. Analytical Letters, 2004, 37, 435-448.	1.0	1
277	Development and application of a fluorescent sensor for potassium ions based on a calix[6]arene ionophore and a novel cationic dye. Supramolecular Chemistry, 2009, 21, 747-753.	1.5	1
278	Chiral discrimination and enantiomeric composition analysis of quinine and quinidine based on paper substrate room temperature phosphorescence. Analytical Methods, 2012, 4, 3928.	1.3	1
279	Development of cryptophane A-coated SAW methane gas sensor. , 2015, , .		1
280	Near-infrared photoluminescence enhancement of N-acetyl- <scp>l</scp> -cysteine (NAC)-protected gold nanoparticles via fluorescence resonance energy transfer from NAC-stabilized CdTe quantum dots. RSC Advances, 2016, 6, 88042-88049.	1.7	1
281	Study on Electrochemical Behavior of Methane at Nickel Electrode Modified with Nickel Hydroxide in Alkaline Solution. , 2007, , .		0
282	STUDY ON THE INTERACTION BETWEEN METHYL BLUE AND HSA IN THE PRESENCE OF \hat{l}^2 -CD/HP- \hat{l}^2 -CD BY MOLECULAR SPECTROSCOPY. , 2008, , .		0
283	Synthesis of La <inf>1−x</inf> Ca <inf>x</inf> FeO <inf>3</inf> nanoparticle by microwave-gel method and its application in photocatalytic degradation of reactive brilliant blue X-BR. , 2011, , .		0
284	Spectroscopic study on the inclusion complexation of L-tyrosine by <i>p</i> -sulphonatocalix[6]arene at different pH values. Physics and Chemistry of Liquids, 2012, 50, 652-660.	0.4	0
285	SYNTHESIS OF A NOVEL FLUORESCENCE PROBE OF ß-CD AND CUPROUS IODIDE PYRIDINE AND ITS APPLICATION. , 2008, , .		0